DYNAMICS OF FLAT BUNCHES WITH SECOND HARMONIC RF*

T. Sen[†], C.M. Bhat, H.J. Kim, J-F. Ostiguy, FNAL, Batavia, IL 60510, USA

Abstract

We investigate the dynamics of longitudinally flat bunches created with a second harmonic cavity in a high energy collider. We study Landau damping in a second harmonic cavity with analytical and numerical methods. The latter include particle tracking and evolution of the phase space density. The results are interpreted in the context of possible application to the LHC.

INTRODUCTION

A possible path to a luminosity upgrade at the LHC is through the creation of longitudinally flat bunches. They can increase the luminosity roughly by 40% when the beam intensities are at the beam-beam limit. Lower momentum spread which can reduce backgrounds and make collimation easier as well lower peak fields which can mitigate electron cloud effects are other advantages. Use of a second harmonic rf system is a frequently studied method to create such flat bunches. Here we consider some aspects of longitudinal dynamics of these bunches in the LHC at top energy. First we consider intensity limits set by the loss of Landau damping against rigid dipole oscillations. Next we describe numerical simulations using both particle tracking and evolution of the phase space density. These simulations address the consequences of driving a bunch at a frequency that corresponds to the maximum of the synchrotron frequency.

RF WITH TWO HARMONICS

We choose the voltage to be of the form

$$V(\phi) = V_{RF}[\sin\phi + k\sin n(\phi - \phi_s)] \qquad (1)$$

where k is the ratio of the higher harmonic ($=n$) voltage to the voltage of the fundamental harmonic. The energy gain per turn of the synchronous particle is the same as if only the fundamental harmonic cavity were present. The potential function is $U(\phi) = \int_0^\phi V(\phi')d\phi'$. The ratio of the stationary bucket area in the second harmonic system relative to that of the single harmonic system is

$$\frac{A_{buck}(k, \phi_s = \pi)}{A_{buck}(k = 0, \phi_s = \pi)} = \frac{1}{2}[\sqrt{1 + 2k} + \frac{\text{Arcsinh}(\sqrt{2k})}{\sqrt{2k}}] \qquad (2)$$

This ratio increases monotonically with k, e.g. at $k = 1/2$, the ratio is 1.15. There is no change in the bucket acceptance for a stationary second harmonic bucket.

Beam Distribution and Beam Induced Voltage

Consider a general binomial distribution $\rho(W, \phi) \propto [H_b - H]^p$ where H is the Hamiltonian and H_b is its value

at the bunch boundary. The line density is the projection on the ϕ axis, $\lambda(\phi) = \lambda_0[U(\phi) - U(\phi_2)]^{p+1/2}$ A special case of this distribution is the elliptic distribution $\rho(W, \phi) \propto \sqrt{H_b - H}$ which was first considered by Hofmann and Pedersen [1]. This has the special feature that the line density is proportional to the potential. Let ϕ_1, ϕ_2 denote the phases at the ends of the bunch. Then the line charge density is

$$\begin{aligned}\lambda(\phi) &= -\frac{N_b}{f}[\cos\phi_2 - \cos\phi + (\phi_2 - \phi)\sin\phi_s \\ &\quad + \frac{k}{n}(\cos n(\phi_2 - \phi_s) - \cos n(\phi - \phi_s))] \end{aligned} \qquad (3)$$

where the function $f(\phi_1, \phi_2)$ is determined by the normalization condition $\int d\phi\lambda(\phi) = N_b$. For a full stationary bucket $f(0, 2\pi) = -2\pi(1 + k/2)$.

Assuming that the effective coupling impedance is mostly reactive, $Z_{eff}(\omega)/n = i[\omega_0 L - g_0 Z_0/(2\beta\gamma^2)]$ where $n = \omega/\omega_0$. For a circular beam of radius a in a circular beam pipe of radius b, $g = 1 + 2\ln(b/a)$. Including the induced voltage, the total voltage is

$$V_t(\phi) = V(\phi) + \frac{2\pi h^2 I_{b,av}\text{Im}(Z_{eff}/n)}{V_{RF}f(\phi_1, \phi_2)}[V(\phi) - V(\phi_s)] \qquad (4)$$

The relative change in the total focusing voltage is given by the factor k_t is $k_t = (V_t(\phi) - V(\phi_s))/(V(\phi) - V(\phi_s)) = 1 + 2\pi h^2 I_{b,av}\text{Im}(Z_{eff}/n)/(V_{RF}f(\phi_1, \phi_2))$. The new potential function is $U_t(\phi) = k_t U(\phi)$. while the net area and synchrotron frequency are reduced by $\sqrt{k_t}$.

LANDAU DAMPING THRESHOLD

The maximum intensity that can be accelerated is given by the condition that the beam induced voltage reduces the bucket area to zero.

$$N_{b,max} = -\frac{1}{e\omega_0 h^2}\frac{V_{RF}}{\text{Im}(Z_{eff}/n)}f(\phi_T, \phi_u) \qquad (5)$$

where ϕ_T, ϕ_u are the bucket endpoints. The frequency of coherent dipole oscillations is found to be

$$\omega_c = \omega_0\sqrt{\frac{h|\eta|}{2\pi}\frac{eV_{RF}}{\beta^2 E_s}}\sqrt{\frac{g(\phi_1, \phi_2)}{|f(\phi_1, \phi_2)|}} \qquad (6)$$

where $g(\phi_1, \phi_2) \equiv 1/(V_{RF}^2)\int_{\phi_1}^{\phi_2}(\partial U/\partial\phi)^2 d\phi$. Let the maximum synchrotron frequency ω_s be ω_s^{max}. The condition for the loss of Landau damping against rigid dipole oscillations is that $\omega_c \geq \omega_s^{max}$, the threshold intensity for this is

$$\frac{N_{b,Landau}}{N_{b,max}} = [\frac{f(\phi_1, \phi_2)}{f(\phi_T, \phi_u)} - \frac{\text{sgn}(\text{f}(\phi_1, \phi_2))}{f(\phi_T, \phi_u)}\frac{g(\phi_1, \phi_2)}{(\bar{\omega}_s^{max})^2}] \qquad (7)$$

05 Beam Dynamics and Electromagnetic Fields
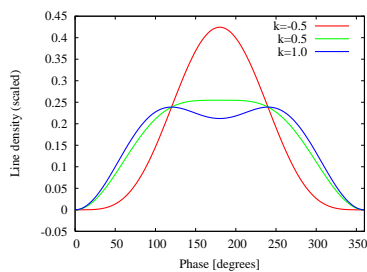
Figure 1: The scaled line density $\lambda/(N_b/2\pi)$ of a bunch filling a stationary bucket with 3 values of k. The flattest profile is at $k = 1/2$.
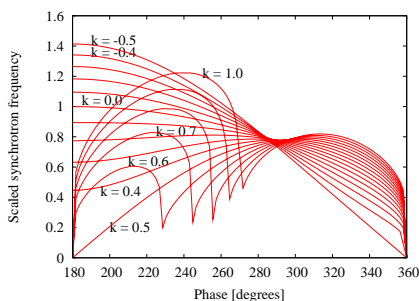
Figure 2: Scaled synchrotron frequency $\bar{\omega}_s$ with a 2nd harmonic rf in a stationary bucket with $-1/2 < k < 1$.

where sgn is the sign function. The synchrotron frequency in the second harmonic system scaled by the frequency at small amplitude in a single harmonic system is obtained from

$$\bar{\omega}_s(\phi_b)^{-1} = \int_{\phi_a}^{\phi_b} \frac{d\phi}{\sqrt{|(\cos\phi_b - \cos\phi)[1 + k(\cos\phi_b + \cos\phi)]|}} \quad (8)$$

Figure 2 shows the scaled synchrotron frequency $\bar{\omega}_s$. When $k \leq 0$, the frequency decreases monotonically with amplitude. When $k \leq 0.5$ the frequency at the center drops with increasing k as $\sqrt{1 - 2k}$ and vanishes when $k = 1/2$. For larger k, the frequency at the center is zero due to the inner separatrix which has an unstable fixed point at π. The frequency has a local maxima at the stable fixed points. Another maximum exists in the range 295-320 degrees for $k > 1/2$. The maximum frequency f_s^{max} for $k = 1/2$ is 17.915 Hz for LHC parameters. The inner separatrix also leads to a sharp cusp in the frequency at a phase amplitude where the inner separatrix crosses the phase axis.

We now calculate the threshold at which Landau damping is lost in the LHC assuming $Z_{ind}/n = 0.1$ Ohms. The left figure in Fig 3 shows the coherent and maximum incoherent synchrotron frequencies including the effect of the inductive impedance and space charge as a function of the voltage ratio k with bunch intensity $N_b = 10^{11}$. The maximum incoherent frequency is above the coherent frequency except in the range $0.55 < k < 0.67$. showing that Landau damping would be lost at this intensity and these k values. The right plot in Fig 3 shows the threshold intensity at
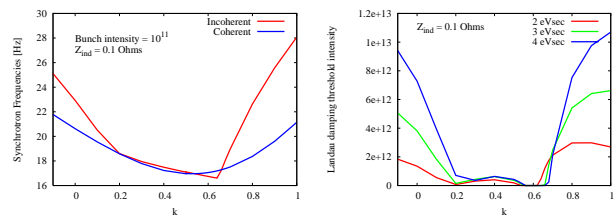
Figure 3: Left: Maximum incoherent and coherent frequency vs the voltage ratio k for nominal LHC parameters. Right: Intensity at which Landau damping is lost vs k at different emittances.

which Landau damping is lost as a function of k for different emittances. The threshold is above the design intensity of 10^{11} until $k = 0.54$ but Landau damping is lost even at zero intensity when $0.56 \leq k \leq 0.67$. At $k = 0.5$ and $\epsilon_L = 3$ ev-sec, the threshold is 3.6×10^{11} which is beyond design intensities at the LHC.

NUMERICAL SIMULATIONS

Experiments in the SPS with a fourth harmonic rf system showed a strong coherent response in the beam transfer function at a frequency corresponding to f_s^{max} [2]. We consider the beam response to an external forced oscillating at this frequency. We use two different simulation methods: a) particle tracking with the code ESME [3], b) evolution of the density with a code developed for this purpose. The simulations reported here were done with $k = 0.5$.

ESME Simulations

The multi-particle longitudinal beam dynamics code ESME [3] is used. The bucket is populated according to the Hoffman-Pedersen distribution with about 35,000 macroparticles. The impedance and the space charge forces are turned on adiabatically and an additional 80 synchrotron periods are allowed to reach equilibrium. Next an external rf drive at a frequency= 17.915 Hz and 0.1 MV amplitude is turned on. This amplitude may be too large but it is about the same as the induced voltage at the bunch edges. The bunch evolution is monitored for the next 60 seconds.

The centroid is observed to oscillate (see Fig 4) at the drive frequency but the amplitude modulates at a beat frequency equal to the difference in frequencies between the drive and the coherent oscillation. From the beat frequency (0.319 Hz), we find the coherent frequency in this case to be 17.606 Hz compared with the estimate of 17.876 Hz using Eq (6). This small discrepancy (1.5%) can however affect the prediction of when Landau damping may be lost. The rms emittance growth corresponding to three different bunch lengths are also shown in Figure 4. The emittance increase is largest for the bunch (1.01 eV-sec) whose phase extent just matches the phase location (297 degrees) of ω_s^{max}. The increase is smaller for the longer bunch which extends up to 330 degrees. After reaching a maximum, the emittance oscillates with a frequency equal to twice the beat frequency of the centroid oscillations before settling
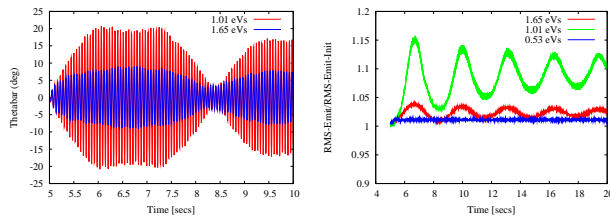
Figure 4: ESME simulations when the beam is driven at a frequency f_s^{max}. Left: Centroid motion for two different emittances. Note the beating motion in both cases. Right: Emittance growth (normalized) for different emittances.
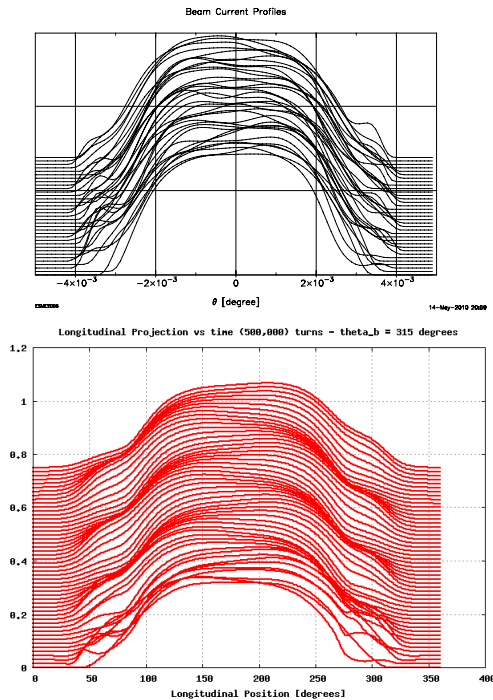
Figure 5: Mountain range view of the line density. Top: ESME simulation with $\epsilon_L = 1.01$eV-sec. Bottom: Vlasov simulation for a longer bunch. Note the development of shoulders in both profiles.

down to an equilibrium value. Neither growth nor oscillations are seen for the shortest bunch length whose phase extent (270 degrees) does not reach the location of ω_s^{max}. Figure 5 shows a mountain range plot of the bunch profile for the bunch with largest emittance growth. A shoulder develops in the profile, similar to that seen in the SPS experiments [2].

Vlasov Simulations

Particle tracking, while conceptually simple, does not resolve well the tails of the beam distribution where there are few particles. An alternative is to adopt the Eulerian point of view, i.e. focus on specific locations in phase space as time evolves or equivalently solve the Vlasov equation. In
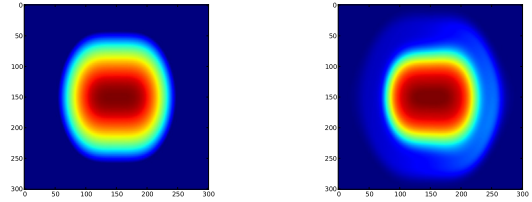
Figure 6: Vlasov simulation of the phase space density for a bunch with $\epsilon_L = 1$ ev-sec and phase extent to 295 degrees.. Left: initial, Right: final distribution after 45 secs develops a halo.

contrast to particle tracking, all locations in phase space are monitored in time and treated on equal footing. Rather than solving the Vlasov partial differential equation, we follow the approach in reference [4] where a semi-Lagrangian technique is used. Symplectic maps are used to ensure long-term preservation of the phase space density. The density distribution is interpolated on a 2D regular rectangular grid using $\mathcal{C}$, third order Lagrange polynomials. At each step in time, the density is updated using the prescription $F(q, p, t_n) = F(\mathcal{M}^{-1}(q, p, t_{n-1}))$ where $\mathcal{M}^{-1}$ represents the inverse of the forward map from t_{n-1} to t_n. The maps are implemented as localized kicks and are applied every turn. Currently, the code can model arbitrary rf cavity waveforms, linear or non linear phase slippage as well as longitudinal impedances and space charge effects. In a typical simulation over 0.5×10^6 turns, on a grid with 10^4 third order cells, we observe less than 10^{-3} variation in the integral of the phase space density.

Results from this Vlasov code are similar to those from ESME. Centroid oscillations show the same beating period and emittance growth is also about the same. Fig 5 shows the mountain range profile of a bunch. Fig 6 shows an example of the phase space distribution at the start and end of about 1000 synchrotron periods. Here the bunch extends to the location of ω_s^{max} and develops a halo due to the excitation. Bunches longer than 340 degrees or shorter than 270 degrees experience very little emittance growth.

To summarize, we have found that voltage ratios between 0.55-0.68 may not be suitable if Landau damping is to be preserved in a second harmonic cavity. Numerical simulations have shown that bunches with phase extent shorter or much longer than the location of the maximum synchrotron frequency experience very little emittance growth when driven at this frequency.

We thank Jim MacLachlan for help with ESME.

REFERENCES

[1] A. Hofmann and F. Pedersen, IEEE Trans. Nuc. Sci. **NS-26**, 3526 (1979).

[2] E. Shaposhnikova et al., PAC 2005, pg 2309 (2005).

[3] J. A. MacLachlan, HEACC98, 184, (1998).

[4] R. Warnock & J. Ellison, in The Physics of High Brightness Beams (World Scientific, Singapore, 2000).